Vol 17 No 5, May 2008
1674-1056/2008/17(05)/1874-07

Chinese Physics B

© 2008 Chin. Phys. Soc.
and IOP Publishing Ltd

Electronic structures and magnetoelectric properties of tetragonal $BaFeO_3$: an *ab initio* density functional theory study*

Feng Hong-Jian(冯宏剑)† and Liu Fa-Min(刘发民)

School of Science, Beijing University of Aeronautics and Astronautics, Beijing 100083, *China*

(Received 8 August 2007; revised manuscript received 12 November 2007)

First-principles calculations have been performed to investigate the ground state electronic properties of $BaFeO_3$ (BFO). Local spin density approximation (LSDA) plus U (LSDA+U) treatment modified the metallic behaviour to insulated one with a band gap of 4.12 eV. The spontaneous polarization was found to be $89.3\mu C/cm^2$ with Berry phase scheme in terms of the modern theory of polarization. Fe-3d e_g were split into two singlet states (d_{z^2} and $d_{x^2-y^2}$), and Fe-3d t_{2g} were split into one doublet states(d_{xz} and d_{yz}) and one singlet states(d_{xy}) after Fe and O displaced along the c axis. Meanwhile the occupation numbers of d_{z^2}, d_{xz}, d_{yz} and O_T p_z (on the top of Fe) were increased at the expense of those in xy plane. Our results showed that it was the sensitivity of hybridization to ferroelectric distortions, not just the total change of hybridization, that produced the possibility of ferroelectricity. Moreover, the increasing occupation numbers of O_T p_z and Fe d_{z^2} favoured the 180° coupling between Fe-3d e_g and Fe-3d t_{2g}, leading to ferromagnetic ordering, which has been confirmed by the increase of magnetic moment by $0.13\mu_B$ per formula unit in the polarized direction. Hence, the magnetization can be altered by the reversal of external electric field.

Keywords: multiferroic, density functional theory, density of states, band structures
PACC: 7115, 7510, 7780

1. Introduction

Multiferroic materials have attracted much interest in recent years for their possessing magnetic order and ferroelectricity in the same phase. Since the 1960s various review articles have systematically classified their properties and behaviours.[1−4] Previous researches showed that the magnetoelectric property originated from the coupling between ferroelectric and ferromagnetic order parameters.[5−9] Even now the driving mechanism of the magnetoelectric multiferroics has not been discovered totally. More investigations on the theoretical methods are needed for the practical applications of these fascinating materials.

$BaFeO_3$ (BFO) has been expected to be a potential magnetoelectric material due to its ferromagnetic ordering of Fe^{4+} ions, and it was reported that it has a hexagonal structure in the bulk form. Recently, Taketani and his collaborators[10] have reported that the epitaxially grown BFO thin films on (100) $SrTiO_3$ substrate with a tetragonal structure might be a potential candidate in multiferroics. Therefore we might regard the BFO with a tetragonal perovskite structure in the bulk form as an ideal candidate for multiferroics. Many perovskite materials have been investigated in terms of the density functional theory.[11−13] One of the first theoretical investigations in $BaTiO_3$ ferroelectric transition has been done by Cohen and Krakouer[14,15] in the early 1990s using the first principles calculations based on the density functional theory (DFT) by local density approximation (LDA) method. Since then, much work has been done for perovskite ferroelectrics such as $SrTiO_3$ and $PbTiO_3$. However, few works have been done on the tetragonal BFO up to now, partly due to the failure in obtaining an insulated bulk. This disadvantage can be overcome by adopting the LSDA+U method. In this paper, electronic properties of BFO in bulk form with tetragonal structure have been systematically investigated, using the first principles calculation based on local density approximation plus U(LSDA+U) method, which can improve the result of insulating properties obtained. We mainly focus on the calculations of the band structures, density of states(DOS), and the change of hybridization of Fe-3d and O-2p states in polarized di-

*Project supported by the Aeronautical Science Foundation of China (Grant No 2003ZG51069).
†Corresponding author. E-mail: fenghongjian@ss.buaa.edu.cn

rection to provide a comprehensive understanding on BFO with this specific tetragonal structure.

The remainder of this paper is organized as follows. First, in Section 2, we present the computational details of our calculations. Then, in Section 3, we report the calculated results and discussion. In Section 4, the conclusions based on our calculation are given.

2. Computational details

2.1. Description of method used

Calculations in this work have been done using the Quantum-ESPRESSO package,[16] which is based on the density functional theory(DFT) in the plane-wave pseudopotential formalism. In our DFT computations, we used our self-interaction-corrected ultrasoft pseudopotential, since the common local density approximation failed to obtain a band gap in the transition metal oxides. Plane-wave basis set with a kinetic energy cutoff of 40 Ry was employed. It is shown that the results are well converged at this cutoff. Ba-5p, Ba-6s, Fe-3s, Fe-3p, Fe-3d, O-2s, and O-2p electrons have been treated as in valence states. We used up to $8\times8\times8$ grids of special k points in total energy calculation. Structural relaxations were performed by minimization of the Hellman–Feynman forces within a convergency threshold of 10^{-3} Ry/Bohr. The energy of a large k-point set was interpolated using the linear tetrahedron method throughout the irreducible Brillouin zone to produce high precision for DOS calculation. Occupation numbers for the orbital-resolved DOS were obtained by integrating the DOS up to the Fermi energy.

Since it is known that LSDA often underestimates the size of the band gap in systems with strong localized orbitals, and sometimes predicts metallic behaviour for insulators. In the LSDA+U framework, the strong Coulomb repulsion is treated by adding a Hubbard-like term to the effective potential, so as to obtain an improved description of the interaction in the transitional metal oxides.[17,18]

2.2. Structure optimization

The optimization of lattice constant was performed under the condition of lowest energy. In this process the structure was kept to be a cubic perovskite. The calculated lattice constants were plotted with respect to total energy and fitted to the Murnaghan equation of states, which gives the bulk modulus.[19] Then the ratio of c/a was changed from 0.70 to 1.05 in steps of 0.01 to produce the minimum energy as the optimal lattice constant was fixed under the constraint of space group $P4mm$. Next, the atomic positions were relaxed freely using Broyden–Fletcher–Goldfarb–Shanno (BFGS) variable metric method with cell shape and volume being fixed.

The antiferromagnetic (AFM) (with neighbouring layers antiparallel to each other) and ferromagnetic (FM) structures were constructed with supercells each having atoms up to 20. Calculated total energy shows that the AFM supercells have a relatively high energy of 0.03eV per unit cell as compared with the FM ones. Hence, in the following we choose the FM ordering as the stable state.

2.3. Spontaneous polarization

In the modern theory of polarization, the total polarization $\boldsymbol{P}$ for a given crystalline geometry can be calculated as the sum of ionic and electronic contributions.[20−22] The ionic contribution is calculated by summing the products of the position of each ion in the unit cell with the nominal charge of its rigid core, while the electronic contribution is determined by evaluating the phase of the product of overlaps between cell-periodic Bloch functions in k-space. We selected a series of seven equally spaced points along the third reciprocal lattice direction in k-space to calculate the electronic contributions to the polarization.

3. Results and discussion

The optimization of volume of a simple cubic lattice was performed with lattice constants ranging from 0.3940nm to 0.4080nm. The lattice parameters versus energy is shown in Fig.1. The calculated values was fitted to the Murnaghan equation of states, and the normal parabolic curve gives the optimal value of 0.4020nm as compared with the experimental value of 0.4021nm for tetragonal BFO thin film.[10] Next, c/a varying from 0.70 to 1.05 is evaluated for total energy at the optimal lattice parameter of 0.4021nm. The c/a vs total energy is depicted in Fig.2. It can be seen that the total energy decreases generally as c/a approaches 0.90 from less than 0.90. While the total energy decreases sharply as c/a approaches 1. This may partly reflect that the tetragonal structure is the stable state, and there might be a phase transition

as c/a approaches 0.90. The optimum value of c/a is found to be 1.025, which agrees well with the experimentally observed values in Ref.[10]. The lattice parameters calculated and those observed experimentally are shown in Table 1. Then the atoms are allowed to move freely with the volume and cell shape being fixed. So the results show that there are smaller deviations of atomic positions in x and y directions, and the displacements of Fe and O along the c axis change with a magnitude of 1% lattice constant.

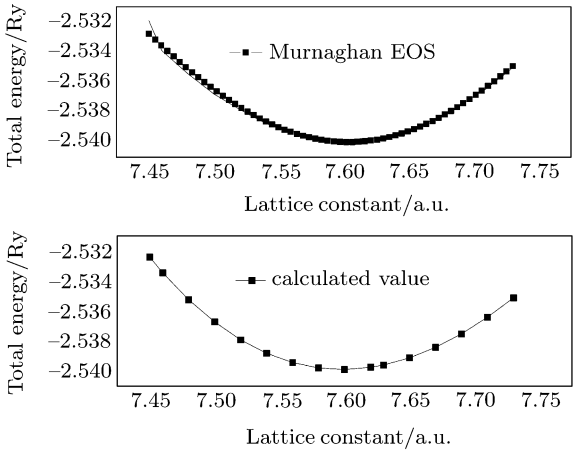


Fig.1. Lattice constant vs energy.

Table 1. The calculated lattice parameter and c/a ratio compared with the experimental values.

	Theor.	Expt.[10]
a/nm	0.4020	0.4021
c/a	1.0025	1.0024

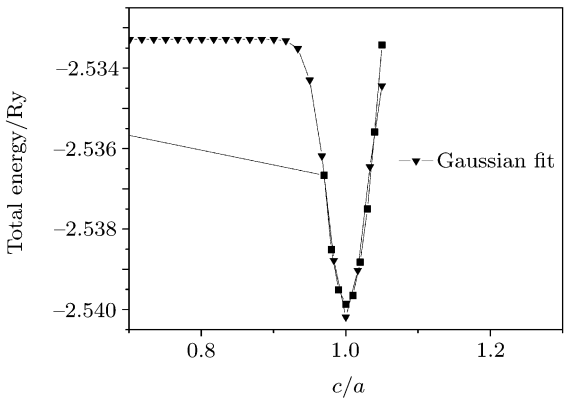


Fig.2. c/a ratio vs energy.

For the simple system consisting of N atoms, by transforming the total Hamiltonian into Wannier representation for the narrow band case, we have

$$H = \sum_{i,j}\sum_{\delta} T_{ij} C^{+}_{i\delta} C_{j\delta} + \frac{1}{2}\sum_{i,j,l,m}\sum_{\delta,\delta'} < ij|v|lm > C^{+}_{i\delta} C^{+}_{j\delta'} C_{m\delta'} C_{l\delta}, \tag{1}$$

where the second term is the interaction that can be simplified by considering the short distance effect on one lattice or atom as follows:

$$\frac{1}{2}U\sum_{i}\sum_{\delta,\delta'} C^{+}_{i\delta} C^{+}_{i\delta'} C_{i\delta'} C_{i\delta} = \frac{1}{2}U\sum_{i}\sum_{\delta} n_{i\delta} n_{i\bar{\delta}}. \tag{2}$$

In Eq.(2) $n_{i\delta}$ and $n_{i\bar{\delta}}$ are the operators of up-spin and down-spin numbers of particles, respectively. Here U is represented by the following formula:

$$< ii|v|ii >= e^2 \int \frac{a^{\star}(\boldsymbol{r}-\boldsymbol{R}_i) a^{\star}(\boldsymbol{r}'-\boldsymbol{R}_i) a(\boldsymbol{r}-\boldsymbol{R}_i) a(\boldsymbol{r}'-\boldsymbol{R}_i)}{|\boldsymbol{r}-\boldsymbol{r}'|} \mathrm{d}\boldsymbol{r}\mathrm{d}\boldsymbol{r}'. \tag{3}$$

So, U is the Coulomb interactions between the electrons around the lattice or atom and has a great effect on the metal–insulator transition. Figures 3 and 4 are the band dispersions with U=0 and 5eV,respectively. From Fig.3 one can see that the Fe-3d bands passing through the Fermi level induce the metallic behaviour of BFO. When a Hubbard-like parameter is applied, the interaction between Fe-3d orbitals would be modified. We used U varying from 0 to 8eV in this work. Since the band gap does not increase significantly as U is greater than 5eV, all the calculations in the following sections will be carried out with U=5eV.

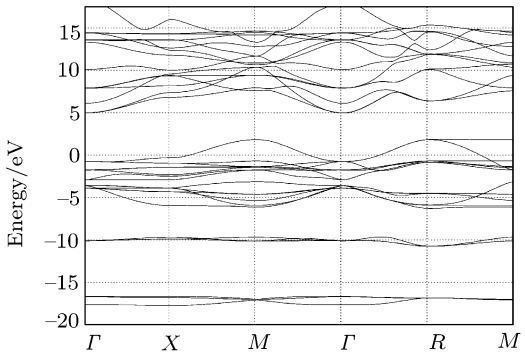


Fig.3. Band dispersions of the FM BFO within LSDA.

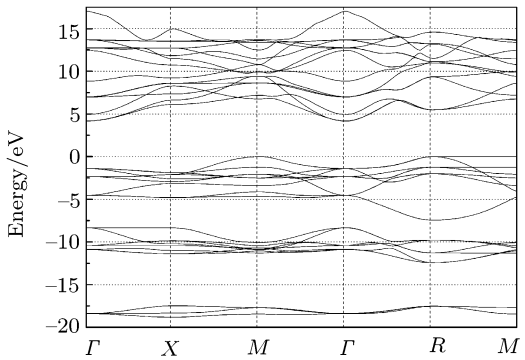


Fig.4. Band dispersions of the FM BFO with U=5eV within LSDA+U scheme.

From the band dispersions shown in Figs.3 and 4, it can be seen that the most distinct dispersion position is at the X point along the Brillouin zone. Moreover, the topmost point in the valence band (VB) is located at R point, and the lowest point in the conduction band (CB) is at Γ point. From Fig.4, the indirect band gap is found to be 4.12eV. The quasi-flat band at –17eV originates from the O-2s states, and those at –11eV owe to the Ba-5p states. The strong overlap in the vicinity of the Fermi energy is attributed mostly to the hybridization of O-2p and Fe-3d orbitals.

Spontaneous polarization is an important parameter for the investigation of ferroelectricity. In order to calculate the polarization along the c axis, the Berry phase method in terms of the modern theory of polarization is used to obtain a value of $89.3\mu C/cm^2$. Experimentally, polarization $\boldsymbol{P}$ corresponds to half of the polarization change as the applied field is swept through zero from positive to negative. The Cartesian components of the polarization ΔP_α with respect to the atomic displacements is Born effective charges(BECs). Usually, it is a standard to estimate ΔP_α by summing the atomic displacements and their correspondence of BECs. The relationship between ΔP_α and BECs is expressed as

$$\begin{aligned}\Delta P_\alpha &\cong \sum_{j\beta} \frac{\partial P_\alpha}{\partial \mu_{j\beta}} (\mu_{j\beta} - \mu_{0j\beta}) \\ &= \frac{e}{\Omega} \sum_{j\beta} \boldsymbol{Z}^\star_{j\alpha\beta} \Delta\mu_{j\beta}, \end{aligned} \tag{4}$$

where $\Delta\mu_{j\beta}$ is the displacement of ion j in Cartesian direction β, $\boldsymbol{Z}^\star_{j\alpha\beta}$ is its BEC tensor, and Ω is the unit cell volume. The BEC along [001] is calculated within the density functional perturbation theory, and the displacement along the c axis is chosen to be smaller (1% lattice constant) enough to ensure the validity of linear treatment in Eq.(4). So, the polarization obtained consequently is $90.4\mu C/cm^2$, and this value is of the same order of magnitude as that from the Berry phase scheme.

In order to study the influence in the electronic structures of displacement of Fe and O along c axis, we have systematically investigated the change of the hybridization between Fe 3d and O 2p along the c axis, but have not just concentrated on the total change of hybridization, which is distinguished from previous papers published elsewhere. The DOS of Fe 3d resolved into d_{z^2}, $d_{x^2-y^2}$, d_{xy}, d_{yz}, d_{xz} orbitals are shown in Figs.5 and 6, corresponding to those before and after displacement along c axis, respectively. From Fig.5 the Fe-3d e_g states are denoted by the shaded areas, and one can see that the Fe-3d are degenerated into t_{2g} and e_g states, the former are triplet states and the latter are doublet states. Occupation numbers of t_{2g} and e_g for centrosymmetric structure are given in Table 2. From Fig.6 it can be seen that the Fe-3d e_g states are split into d_{z^2} and $d_{x^2-y^2}$ states with the displacement of Fe and O, which are indicated by the light grey and dark grey areas, respectively. Meanwhile the Fe-3d t_{2g} states are split into d_{yz}, d_{xz}, and d_{xy} states. Note that the d_{yz} and d_{xz} are doublet. The corresponding occupation numbers are listed in Table 3. And the triplet Fe-3d t_{2g} states including d_{yz}, d_{xz}, and d_{xy} have acted as a rigid core charge, which is relatively stable and resist to change from the centrosymmetric structure. Before displacement of Fe and O, occupation numbers of d_{yz}, d_{xz}, and d_{xy} are 0.99 for the up-spin states and 0.14 for the down-spin states, respectively. Meanwhile, the corresponding values for d_{z^2} and $d_{x^2-y^2}$ are 0.93 and 0.32 respectively. After the displacement of Fe and O along c axis, the Fe-3d e_g are split obviously into two singlets (d_{z^2} and $d_{x^2-y^2}$). From Table 3, occupation numbers

of d_{z^2} and $d_{x^2-y^2}$ change to 0.96 and 0.91 respectively. While t_{2g} does not change significantly in terms of its strong core charge effect. So, occupation numbers for down-spin states of d_{yz}, d_{xz} are slightly reduced, and the occupation numbers for up-spin and down-spin states of d_{xy} are not changed. It further proved that the x and y orbitals are insensitive to displacements along c axis. It is these two trends(reorientation in z direction and insensitive behaviour in x, y directions) that make the hybridization balance under destabilizing ferroelectric distortions. It demonstrates that the hybridization between Fe 3d and O_T 2p states leads to the reorientation of hybridization in the c axis. From the change of occupation numbers of different degenerated states, it can be seen that the reorientation of hybridization in the polarized direction is obtained at the expense of the hybridization in the xy plane.

Table 2. Occupation numbers of resolved Fe-3d orbitals. n_{up} and n_{down} are the numbers for up-spin and down-spin states.

	d_{z^2}	d_{xz}	d_{yz}	$d_{x^2-y^2}$	d_{xy}	total
n_{up}	0.93	0.99	0.99	0.93	0.99	4.83
n_{down}	0.32	0.14	0.14	0.32	0.14	1.06

Table 3. Occupation numbers of resolved Fe-3d orbitals after Fe and O are displaced. n_{up} and n_{down} are the numbers for up-spin and down-spin states.

	d_{z^2}	d_{xz}	d_{yz}	$d_{x^2-y^2}$	d_{xy}	total
n_{up}	0.96	0.99	0.99	0.91	0.99	4.84
n_{down}	0.22	0.12	0.12	0.34	0.14	0.94

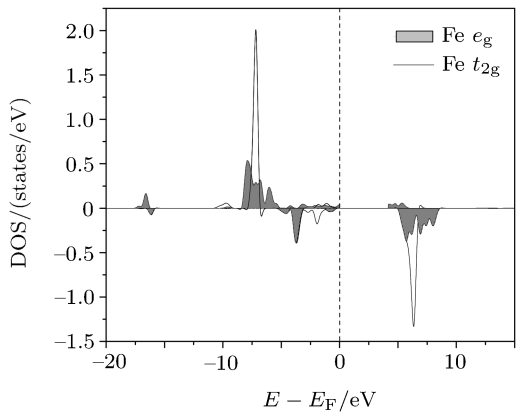


Fig.5. Orbital-resolved DOS of Fe 3d for the centrosymmetric structure. The shaded area indicates the Fe e_g states, and the solid line indicates the Fe t_{2g} states. Vertical line indicates the Fermi energy.

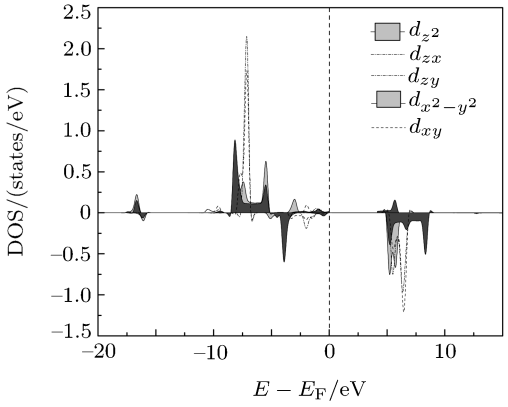


Fig.6. Orbital-resolved DOS of Fe 3d as Fe and O displaced along the c axis. The light grey and dark grey area indicate the Fe d_{z^2} and Fe $d_{x^2-y^2}$ orbitals respectively. The d_{xz}, d_{yz} and d_{xy} orbitals are illustrated with different line styles. Note that the d_{xz} and d_{yz} are doublet. Vertical line indicates the Fermi energy.

From Table 2 and Table 3, the total magnetic moments of Fe are about $3.77\mu_B$ and $3.90\mu_B$ before and after displacements of Fe and O, respectively. Therefore, one can see that the total change of magnetic moment per unit cell is about $0.13\mu_B$, which is mainly attributed to the change of spin in d_{z^2}. It is clear that the large polarization has been achieved, accompanied with the increase of magnetization along the polarized direction.

We considered that the 180° coupling between e_g and t_{2g} electrons are enhanced to induce the FM ordering, accompanied with the kinetic exchange decrease, which is caused by the lowering of the symmetry.[9] From the super-exchange theory, the 180° coupling between e_g and t_{2g} might be achieved by the intermediate oxygen atom. The orbital-resolved DOS of O_T (on the top of the Fe) is shown in Fig.7,

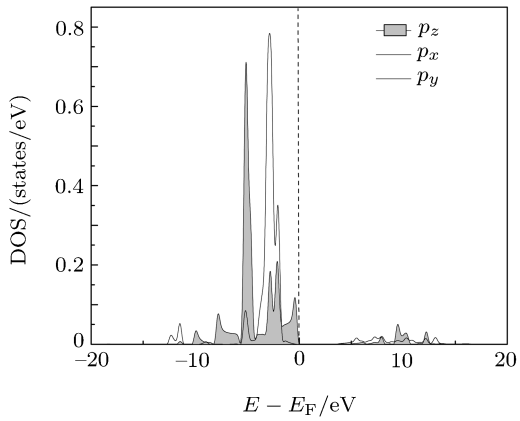


Fig.7. Orbital-resolved DOS of O 2p as Fe and O displaced along the c axis. Shaded area indicates the p_z states. p_x and p_y are doublet. Vertical line indicates the Fermi energy.

from which one can see that the O-2p states are degenerated into one singlet (p_z) and one doublet states (p_x and p_y). Occupation numbers of O_T 2p along the c axis are shown in Table 4 before and after displacements. The displacement induces the up-spin occupation numbers of 0.76 in the O_T p_z states, while the centrosymmetric one only has an occupation number of 0.63. It is in good agreement with the increase of occupation numbers of Fe in the c axis. The change of occupation numbers of Fe and O along the c axis confirms the strong hybridization between Fe and O in the polarized direction. Hence, reorientation of hybridization of Fe and O along the c axis tends to induce a good ferroelectricity. And the increase of occupation numbers of O along the c axis tends to enhance the 180° coupling between Fe 3d e_g and Fe 3d t_{2g}, and further bring about a FM ordering, which can be confirmed by the increase of magnetic moment of Fe in the unit cell.

Table 4. Occupation numbers of resolved O_T 2p orbitals before and after Fe and O displaced. n_{up} and n_{down} are the numbers for up-spin and down-spin states.

	centrosymmetric structure			Fe and O displaced along c axis		
	p_z	p_x	p_y	p_z	p_x	p_y
n_{up}	0.63	0.87	0.87	0.76	0.88	0.88
n_{down}	0.71	0.82	0.82	0.81	0.87	0.87

The fascinating characteristics of magnetoelectric materials are attributed to the rotation of magnetization induced by reversal of external electric field. While the coupling between the magnetism and ferroelectricity involves not only the super-exchange interaction but also the spin-orbit interaction. The Hamiltonian of magnetoelectric system can be written as

$$\tilde{H} = \tilde{H}^{E} + \tilde{H}^{M} + \tilde{H}^{EM}, \tag{5}$$

where the superscripts E, M and EM represent the electric subsystem part, the magnetic subsystem part and the coupling term between them, respectively. In this specific tetragonal BFO, as an external electric field is applied in z-direction, the displacement along the polarized direction (c axis) is induced by the accompanying of the magnetic configuration rearrangement. Therefore, the reversal of external electric field can lead to the change of magnetic configuration, and it results in the rotation of magnetization. Moreover, the coupling can be achieved by the interaction between ferromagnetism and structural distortions in the system. In the classic mutiferroic $BiFeO_3$, the resulting magnetization can be altered by the reversal of sense of rotation of the neighbouring oxygen octahedra along [111]. Unfortunately, the resulting magnetization in $BiFeO_3$ have been cancelled significantly in the G-type antiferromagnetic configuration. Fortunately, in BFO the coupling between the ferromagnetism and structural distortions has been achieved in the same phase. The small displacement of Fe and O can bring about the increase of magnetic moment of $0.13\mu_B$ per formula unit along the polarized direction. Hence, the magnetization can be rotated by the reversal of external electric field.

4. Conclusion

By the predicted coexistence of magnetic and ferroelectric behaviour in epitaxially grown BFO thin film on (100) $SrTiO_3$ substrate, first principle calculations on BFO have been performed to investigate the driving mechanism of magnetoelectric properties. The spontaneous polarization is found to have a value of $89.3\mu C/cm^2$. And we have further calculated occupation numbers by integrating the partial DOS of Fe 3d resolved into d_{z^2}, $d_{x^2-y^2}$, d_{yz}, d_{xz}, and d_{xy} states and the O 2p partial DOS resolved into p_z, p_y and p_x states before and after the displacement of Fe and O along the c axis. All of the results show that the hybridization is enhanced in the polarized direction. It is thought that the increase of occupation numbers of O_T p_z is able to enhance the $e_g - t_{2g}$ bonding and further favour a FM ordering. Then the increase of magnetic moment of Fe along the polarized direction after displacement indicates the coupling of ferroelectricity and ferromagnetism. Therefore, the magnetization can be controlled by reversal of external electric field.

References

[1] Skinner S M 1970 *IEEE Trans. Parts, Materials and Packaging* **6** 68

[2] Schmid H 1973 *Int. J. Magnetism* **4** 337

[3] Smolenskii G A and Chupis I E 1982 *Sov. Phys. Usp.* **25** 475

[4] Schmid H 1994 *Ferroelectrics* **62** 317

[5] Ederer C and Spaldin N A 2006 *Curr. Opin. Sol. Stat. and Mater. Sci.* **9** 128

[6] Spaldin N A and Fiebig M 2005 *Science* **309** 391

[7] Duan C G, Jaswal S S and Tsymbal E Y 2006 *Phys. Rev. Lett.* **97** 047201

[8] Neaton J B, Ederer C, Waghmare U V, Spaldin N A and Rabe K M 2005 *Phys. Rev.* B **71** 014113

[9] Baettig P, Ederer C and Spaldin N A 2005 *Phys. Rev.* B **72** 214105

[10] Eiichi Taketani, Toshiyuki Matsui , Norifumi Fujimura and Kenji Morii 2004 *IEEE Trans. Magnetics.* **40** 2736

[11] Wang Y X, Zhong W L, Wang C L, Zhang P L and Su X T 2002 *Chin. Phys.* **11** 0714

[12] Zhang C, Wang C L, Li J C and Yang K 2007 *Chin. Phys.* **16** 1422

[13] Chen S Y, Li Y R, Xue W D and Yang C 2005 *Acta Phys. Sin.* **54** 848 (in Chinese)

[14] Cohen R E and Krakouer H 1990 *Phys. Rev.* B **42** 6416

[15] Cohen R E 1992 *Nature* **358** 136

[16] Baroni S, Dal Corso A, de Gironcoli S, Giannozzi P, Cavazzoni C, Ballabio G, Scandolo S, Chiarotti G, Focher P, Pasquarello A, Laasonen K, Trave A, Car R, Marzari N and Kokalj A http://www.pwscf.org/

[17] Anisimov I Vladimir, Zaanen Jan and Andersen K Ole 1991 *Phys. Rev.* B **44** 943

[18] Cococcioni Matteo and de Gironcoli S 2005 *Phys. Rev.* B **71** 035105

[19] Murnaghan F D 1944 *Pro. Natl. Acad. Sci.* USA **30** 244

[20] King-Smith R D and Vanderbilt D 1993 *Phys. Rev.* B **47** 1651

[21] King-Smith R D and Vanderbilt D 1994 *Phys. Rev.* B **48** 4442

[22] Resta R 1994 *Rev. Mod. Phys.* **66** 899